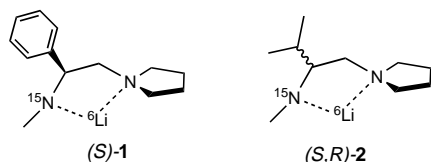


# <sup>6</sup>Li and <sup>15</sup>N NMR Data as a Probe for the Influence of Solvent and Intramolecular Solvation on the Solution-State Structures of Chiral Lithium Amides\*\*

Per I. Arvidsson and Öjvind Davidsson\*

The molecular design of chiral auxiliaries and ligands for use in asymmetric synthesis is of outmost importance in modern organic chemistry. A large variety of chiral ligands has been designed for catalytic or stoichiometric chirality transfer in various reactions.<sup>[1]</sup> Much effort has been put into ligand optimization since the degree of asymmetric induction obtained in a particular system is often critically dependent upon the structure of the organic ligand. Regardless of whether the ligand structure has been optimized through trial and error, through a combinatorial approach, or through computational modeling of a known transition-state structure, is it vital to know the exact composition and structure of the reagent in use. However, the reagent taking part in the reaction is not necessarily the simple monomeric ligand itself. More often, the reagent is composed of aggregated species.<sup>[2]</sup> This is especially true for organometallic reagents.

Here we report multinuclear and multidimensional NMR spectroscopic studies on enantiomerically pure lithium (*S*)-methyl(1-phenyl-2-pyrrolidinoethyl)[<sup>15</sup>N]amide (**1**) and racemic, as well as the enantiomerically pure, lithium (1-isopropyl-2-pyrrolidinoethyl)methyl[<sup>15</sup>N]amide (**2**). These lithium amides display a large diversity of aggregation and coordination abilities.



The <sup>6</sup>Li NMR spectrum of the chiral lithium amide **1**, in diethyl ether ([D<sub>10</sub>]DEE) at  $-90^{\circ}\text{C}$ , displays three groups of signals (Figure 1a). Two triplets, appearing in a 1:1 ratio, are observed at  $\delta = 2.15$  ( $J_{\text{Li},^{15}\text{N}} = 3.7$  Hz) and  $\delta = 2.32$  ( $J_{\text{Li},^{15}\text{N}} = 6.1$ ). Another, less intense triplet is observed at  $\delta = 1.63$  ( $J_{\text{Li},^{15}\text{N}} = 4.5$  Hz). The  $T_1$  values and the linewidths of the signals at  $\delta = 2.15$  and  $2.32$  are notably different: 6.1 s and 0.98 Hz ( $\delta = 2.15$ ), 2.5 s and 2.33 Hz ( $\delta = 2.32$ ). These variations in  $T_1$  and linewidth are in accordance with previous studies of chiral lithium amide dimers reporting a difference in solvation of the two lithium cations. The results indicate that the lithium ion at  $\delta = 2.15$  is tetracoordinated and the lithium ion at  $\delta = 2.32$  is tricoordinated.<sup>[3]</sup> The splitting pattern

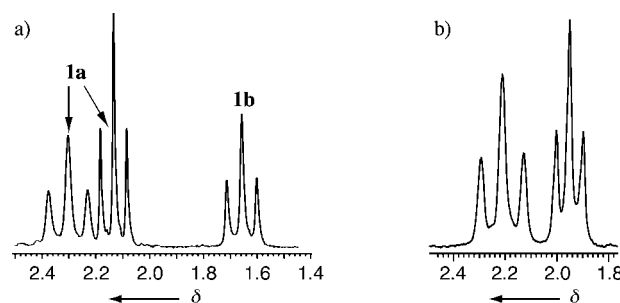
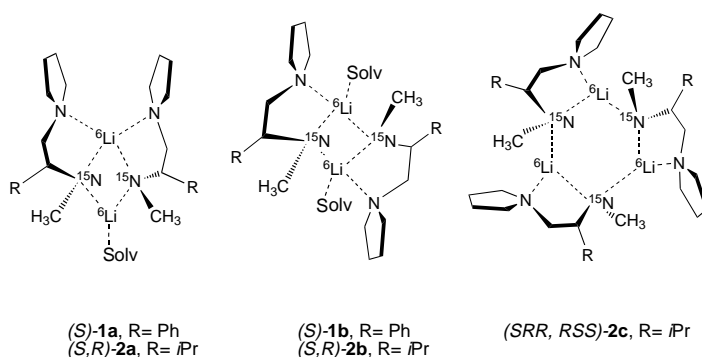


Figure 1. <sup>6</sup>Li NMR spectra of a) **1** at  $T = -90^{\circ}\text{C}$  in [D<sub>10</sub>]DEE, isotopic enrichment <sup>15</sup>N [ $>98\%$ ] and <sup>6</sup>Li [ $95\%$ ], b) **2** at  $T = -70^{\circ}\text{C}$  in [D<sub>10</sub>]DEE, isotopic enrichment <sup>15</sup>N [ $98\%$ ] and <sup>6</sup>Li [ $95\%$ ].

and linewidths, together with a temperature-independent 1:1 integral ratio of the two lithium signals at  $\delta = 2.15$  and  $2.32$ , reveal that these signals originate from an unsymmetrically solvated dimer, that is **1a** in Scheme 1. Unsymmetrically



Scheme 1. Structures of the lithium amides **1** and **2** identified in solution. Solv = solvating ligand.

solvated dimers containing two lithium atoms with different chemical surroundings and coordination have previously been described by us and by others.<sup>[4]</sup> The triplet at  $\delta = 1.63$  was found to increase in intensity with decreasing temperature at the expense of the two other signals. The splitting pattern and the temperature dependence, together with the titration studies presented below, confirm that this resonance originates from a symmetrically solvated dimer, that is **1b** in Scheme 1.

The integrals of the <sup>6</sup>Li NMR signals of **1**, at  $-90^{\circ}\text{C}$  in [D<sub>10</sub>]DEE, show that the unsymmetrically coordinated dimer **1a** is slightly favored over the symmetrically coordinated dimer **1b** under these conditions (integral ratio 70:30; [**1**]<sub>tot</sub> = 0.65 m). Upon addition of THF, the chemical shifts of the resonances originating from **1a** were unaffected; however, the lithium signal of **1b** shifted slightly downfield to about  $\delta = 1.70$  and increased in intensity. The intensity of the <sup>6</sup>Li NMR signals of **1a** continued to decrease when more THF was added. When one equivalent of THF had been added, only the symmetrically coordinated dimer **1b** could be observed. Addition of TMEDA to this solvent mixture did not alter the <sup>6</sup>Li NMR chemical shifts or <sup>6</sup>Li,<sup>15</sup>N coupling constants to any extent—surprisingly, no monomers were formed. Titration of a solution of **1** in DEE at  $-90^{\circ}\text{C}$  with cyclohexene

[\*] Dr. Ö. Davidsson, Dr. P. I. Arvidsson  
Department of Organic Chemistry  
Göteborg University, Göteborg, 412 96 (Sweden)  
Fax: (+46)31-772-3840  
E-mail: ojvind.davidsson@oc.chalmers.se

[\*\*] The authors are most grateful to the Swedish Natural Science Research Council and Carl Trygger for financial support.

oxide, the substrate commonly used to evaluate the efficiency of chiral lithium amide bases in enantioselective rearrangement reactions, showed the same behavior as described above. Only the symmetrically solvated dimer was obtained with a signal around  $\delta = 1.70$ .

In contrast to **1**, the lithium amide **2** in  $[D_{10}]$ DEE at  $-70^\circ\text{C}$  displayed only two triplets at  $\delta = 1.95$  ( $J_{\text{Li},^{15}\text{N}} = 3.8$  Hz) and  $\delta = 2.22$  ( $J_{\text{Li},^{15}\text{N}} = 6.2$  Hz) (Figure 1b). These signals appeared in a 1:1 integral ratio at all temperatures studied. The  $^{15}\text{N}$  NMR spectrum of **2** in  $[D_{10}]$ DEE at  $-70^\circ\text{C}$  showed only one signal at  $\delta = -77.5$ , indicating the presence of only one species in solution. Thus, this lithium amide forms an unsymmetrically coordinated dimer in DEE (**2a** in Scheme 1). The signal of the tetracoordinated lithium ion appears at  $\delta = 1.95$  ( $T_1 = 7.0$  s, linewidth 1.1 Hz), that of the tricoordinated ion at  $\delta = 2.22$  ( $T_1 = 2.0$  s, linewidth 1.7 Hz). The  $^6\text{Li}$  resonances of the DEE-solvated **2a** decreased upon titration with THF, and a new  $^6\text{Li}$  NMR signal appeared at  $\delta = 1.61$  ( $J_{\text{Li},^{15}\text{N}} = 4.5$  Hz). This signal was assigned to a symmetrically solvated species (see above).

The  $^6\text{Li}$  resonances for the unsymmetrically solvated dimer **2a** show similar differences in  $T_1$ , linewidth, and coupling constants as for **1a**. The difference in coupling constants between the tetracoordinated lithium ions ( $J_{\text{Li},^{15}\text{N}} \approx 4$  Hz) and the tricoordinated lithium ions ( $J_{\text{Li},^{15}\text{N}} \approx 6$  Hz) is in good agreement with the results of computational studies by Kikuchi and co-workers.<sup>[5]</sup> This suggests that not only the aggregation state, but also the coordination number at the lithium ion strongly affects the magnitude of the coupling constant. Collum and co-workers have also observed differences in the  $^6\text{Li},^{15}\text{N}$  coupling constants upon changes in solvation of symmetrically solvated lithium amides. However, these differences were assigned to a distortion in the dimer core and not to electronic factors.<sup>[6]</sup> In the unsymmetrically solvated lithium amides reported here, we may directly probe the electronic effects associated with increased or decreased coordination at the lithium atom using  $^6\text{Li},^{15}\text{N}$  coupling constants. These data show that increased coordination at the lithium ion reduces the magnitude of the  $^6\text{Li},^{15}\text{N}$  coupling constant.

The  $^6\text{Li},^{15}\text{N}$  coupling constants of 4.5 Hz observed for the symmetrically coordinated dimers indicate that the lithium atoms in such dimers are mainly tetracoordinated. This conclusion is supported by the temperature dependence of the equilibrium between **1a** and **1b**, as well as the titration studies with THF; in other words, the more solvated dimers **1b** and **2b** are favored at low temperatures and in solvents with a high propensity to coordinate lithium.

A solution of **2** in  $[D_8]$ toluene at  $-70^\circ\text{C}$  displayed three  $^6\text{Li}$  NMR signals of equal intensity at  $\delta = 2.47$  ( $J_{\text{Li},^{15}\text{N}} = 5.9$  Hz), 2.60 ( $J_{\text{Li},^{15}\text{N}} = 5.5$  Hz), and 2.71 ( $J_{\text{Li},^{15}\text{N}} = 5.5$  Hz). The  $^{15}\text{N}$  NMR spectrum of this solution also displayed three signals at  $\delta = -68.5$ ,  $-74.0$ , and  $-77.0$ . These signals were assigned using a  $^6\text{Li},^{15}\text{N}$ -HMQC 2D NMR experiment (Figure 2a). The coupling pattern clearly indicates that the  $^6\text{Li}$  NMR signals originate from one complex, as they show coupling to all  $^{15}\text{N}$  nuclei. Consequently, **2** forms a cyclic trimer (**2c** in Scheme 1) in  $[D_8]$ toluene. The magnitude of the  $^6\text{Li},^{15}\text{N}$  coupling constant was almost the same (ca. 5.5 Hz) for all lithium ions in the cyclic trimer. This suggests tricoordination; that is each

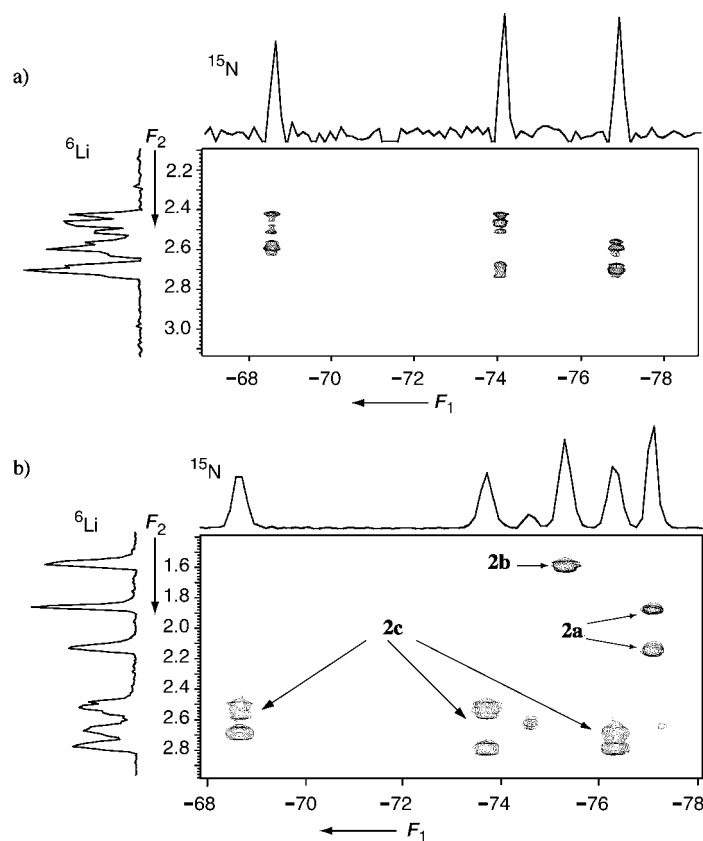


Figure 2.  $^6\text{Li},^{15}\text{N}$ -HMQC 2D NMR spectra of a) **2** at  $-70^\circ\text{C}$  in  $[D_8]$ toluene, b) **2** at  $-70^\circ\text{C}$  in  $[D_8]$ toluene, with 4.0 equiv of  $[D_{10}]$ DEE and 0.6 equiv of  $[D_8]$ THF added; the spectrum shows signals of the aggregates **2a**, **2b**, and **2c** present under these conditions.

pyrrolidine ring coordinates to one lithium atom. Thus, it appears that only one of the possible chelators<sup>[7]</sup> exists under these conditions. Surprisingly, the chiral lithium amide **1** displayed only two main triplets in  $[D_8]$ toluene at  $-70^\circ\text{C}$ . This unexpected result led us to investigate a sample of enantiomerically pure (*R*)-**2**, however *without*  $^{15}\text{N}$  labeling.

As shown in Figure 3a, enantiomerically pure (*R*)-**2** also displays only two main signals, probably originating from an unsymmetrical dimer or from a homochiral trimeric species. However, addition of small amounts of the enantiomer (*S*)-**2** to this solution results in the immediate appearance of the three signals originally seen for racemic **2** (Figure 3b). Further addition of (*S*)-**2**, up to two equivalents, only results in more trimer formation. Addition of more than two equivalents of (*S*)-**2** again leads to the homochiral species (Figure 3c–e). Thus in  $[D_8]$ toluene, these chiral lithium amides display a large tendency to form heterochiral trimers, that is cyclic trimers (*S,R,R*)-**2** or (*R,S,S*)-**2**. The nitrogen atoms in these aggregates are also stereogenic centers. They may undergo rapid inversion or, more likely, the configuration at the nitrogen centers could result from “transfer of chirality” induced by the proximal stereogenic carbon centers.<sup>[8]</sup> Apparently, one of the possible diastereomers is more stable than the others since only one set of signals results.

A careful titration of the original toluene solution of racemic,  $^{15}\text{N}$ -labeled **2** with DEE, THF, and finally TMEDA allowed us to simultaneously prepare all the previously

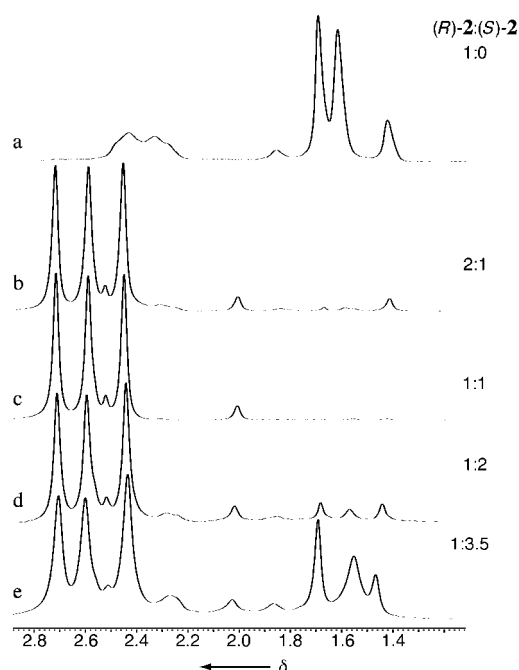


Figure 3.  $^6\text{Li}$  NMR spectra of **2** without  $^{15}\text{N}$  labeling at  $-90^\circ\text{C}$  in  $[\text{D}_8]\text{toluene}$ . a) Enantiomerically pure (*R*)-**2**, b–e) (*R*)-**2** with increasing amounts of (*S*)-**2** added.

described species (Figure 4). The  $^6\text{Li},^{15}\text{N}$ -HMQC 2D experiment of this mixture, prior to addition of TMEDA, is shown in Figure 2b. This spectrum clearly shows the presence of all species described in Scheme 1: the cyclic trimer **2c**, the symmetrically solvated dimer **2b**, and the unsymmetrically solvated dimer **2a**.

To conclude, the lithium amides **1** and **2** form trimers as well as symmetrically and unsymmetrically solvated dimers depending on the solvent used. Trimers are observed for **1** and **2** in hydrocarbon solvents like toluene, at least when an enantiomerically impure reagent is used. The lithium amide **2** forms unsymmetrically solvated dimers in DEE but symmetrically solvated dimers in THF, whereas the lithium amide **1** gives both unsymmetrically and symmetrically solvated dimers in DEE. The temperature-dependent equilibrium between **1a** and **1b** suggests that one additional molecule of DEE is required to form the symmetrically coordinated dimer **1b**. Thus, the different ability of **1** and **2** to form unsymmetrically solvated dimers in DEE is probably a result of the different spacial congestion by the isopropyl and the phenyl group.

Furthermore, we have demonstrated that the coordination number at the lithium ions in **1** and **2** can be monitored by NMR linewidths and  $T_1$  values as well as by the magnitude of the  $^6\text{Li},^{15}\text{N}$  coupling constants. We conclude that the magnitude of the coupling constant is a very sensitive tool for probing changes in the coordination number of lithium ions and, we believe, more reliable than  $T_1$  or the linewidth for determining the coordination number of a lithium ion;  $T_1$  relaxation rates are very sensitive to the aggregation state, whereas effects of aggregation upon  $^6\text{Li},^{15}\text{N}$  coupling constants are less significant.<sup>[9]</sup>

Received: March 15, 1999

Revised: December 6, 1999 [Z13165]

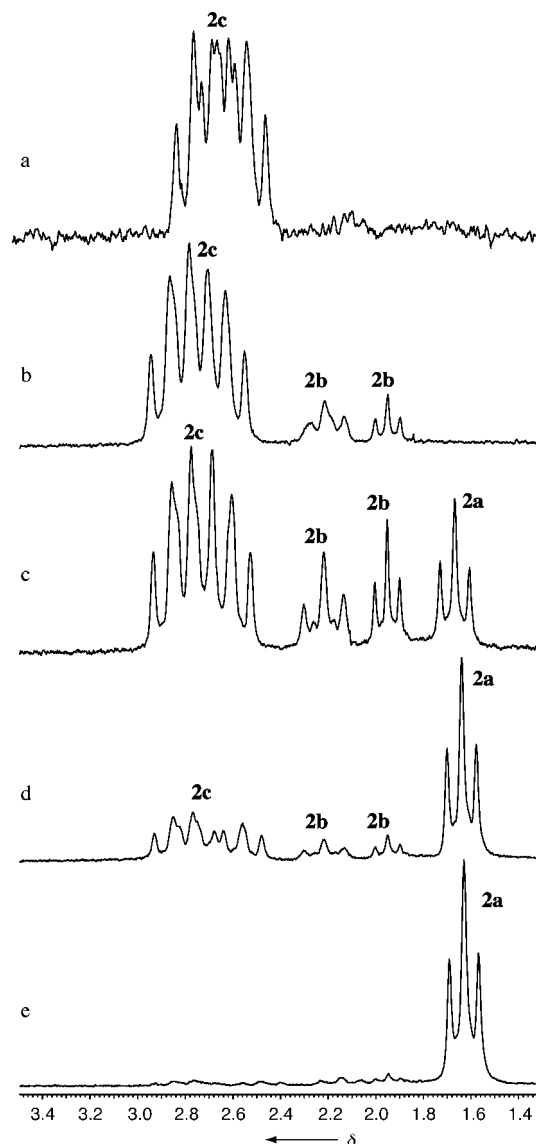


Figure 4.  $^6\text{Li}$  NMR spectra of **2** at  $-70^\circ\text{C}$  in a)  $[\text{D}_8]\text{toluene}$  titrated with b)  $[\text{D}_{10}]\text{DEE}$ , c)  $[\text{D}_8]\text{THF}$ , and d, e) TMEDA.

- [1] D. Lucet, T. Le Gall, C. Mioskowski, *Angew. Chem.* **1998**, *110*, 2724–2772; *Angew. Chem. Int. Ed.* **1998**, *37*, 2580–3627; P. O'Brien, *J. Chem. Soc. Perkin Trans. 1* **1998**, 1439–1456; P. J. Cox, N. S. Simpkins, *Tetrahedron: Asymmetry* **1991**, *2*, 1–26; K. Koga, *J. Synth. Org. Chem. Jpn.* **1990**, *48*, 463–475; K. Koga, *Pure Appl. Chem.* **1994**, *66*, 1487–1492; K. Koga, M. Shindo, *J. Synth. Org. Chem. Jpn.* **1995**, *52*, 1021–1032; P. Beak, A. Basu, D. J. Gallagher, Y. S. Park, S. Thayumanavan, *Acc. Chem. Res.* **1996**, *29*, 552–560; D. Hoppe, *Angew. Chem.* **1997**, *109*, 2376–2410; *Angew. Chem. Int. Ed. Engl.* **1997**, *36*, 2282–2316.
- [2] W. Setzer, P. von R. Schleyer, *Adv. Organomet. Chem.* **1985**, *24*, 353–451; U. Olsher, R. M. Izatt, J. S. Bradshaw, N. K. Dalley, *Chem. Rev.* **1991**, *91*, 137–164; R. E. Mulvey, *Chem. Soc. Rev.* **1991**, *20*, 167–209; K. Gregory, P. von R. Schleyer, R. Snaith, *Adv. Organomet. Chem.* **1991**, *37*, 47–142; G. Fraenkel, M. Henrichs, J. M. Hewitt, B. M. Su, M. Geckle, *J. Am. Chem. Soc.* **1980**, *102*, 3345–3350; D. Seebach, R. Hässig, J. Gabriel, *Helv. Chim. Acta* **1983**, *66*, 308–337; H. Günther, D. Moskau, P. Bast, D. Schmalz, *Angew. Chem.* **1987**, *99*, 1242–1249; *Angew. Chem. Int. Ed. Engl.* **1987**, *26*, 1212–1220; W. Bauer, P. von R. Schleyer, *Advances in Carbanion Chemistry*, Vol. 1 (Ed.: V. Snieckus), JAI, Greenwich, CT, USA, **1992**, pp. 89–175; "Advanced Application of NMR to Organometallic Chemistry": H. Günther in *Physical Organometallic Chemistry*, Vol. 1 (Eds.: M. Gielen, R. Willem, B. Wrackmeyer), Wiley, Chichester, **1996**, pp. 247–290.

- [3] G. Hilmersson, Ö. Davidsson, *J. Org. Chem.* **1995**, *60*, 7660–7669.
- [4] G. Hilmersson, P. I. Arvidsson, Ö. Davidsson, M. Håkansson, *Organometallics* **1997**, *16*, 3352–3362; G. Hilmersson, P. I. Arvidsson, Ö. Davidsson, M. Håkansson, *J. Am. Chem. Soc.* **1998**, *120*, 8143–8149; P. I. Arvidsson, G. Hilmersson, P. Ahlberg, *J. Am. Chem. Soc.* **1999**, *121*, 1883–1887; H. J. Reich, B. Ö. Gudmundsson, *J. Am. Chem. Soc.* **1996**, *118*, 6074–6075; H. J. Reich, D. P. Green, M. A. Medina, W. S. Goldenberg, B. Ö. Gudmundsson, R. R. Dykstra, N. H. Phillips, *J. Am. Chem. Soc.* **1998**, *120*, 7201–7210; J. S. DePue, D. B. Collum, *J. Am. Chem. Soc.* **1988**, *110*, 5518–5524; B. L. Lucht, D. B. Collum, *J. Am. Chem. Soc.* **1996**, *118*, 2217–2225; B. L. Lucht, M. P. Bernstein, J. F. Remenar, D. B. Collum, *J. Am. Chem. Soc.* **1996**, *118*, 10707–10718.
- [5] T. Koizumi, K. Morihashi, O. Kikuchi, *Bull. Chem. Soc. Jpn.* **1996**, *69*, 305–309.
- [6] F. E. Romesberg, J. H. Gilchrist, A. T. Harrison, D. J. Fuller, D. B. Collum, *J. Am. Chem. Soc.* **1991**, *113*, 5751–5757.
- [7] R. F. Schmitz, F. J. J. de Kanter, M. Schakel, G. W. Klumpp, *Tetrahedron* **1994**, *50*, 5933–5944.
- [8] We are grateful to one of the referees for drawing our attention to this point and plan to investigate this remarkable observation in a full paper. For a review on the transfer of chirality, see H. Buschmann, H.-D. Scharf, N. Hofmann, P. Esser, *Angew. Chem.* **1991**, *103*, 480–518; *Angew. Chem. Int. Ed. Engl.* **1991**, *30*, 477–515, and references therein.
- [9] Note added in proof: In a recent paper Collum's group also attributed a change in  $^{16}\text{Li}$ ,  $^{15}\text{N}$  coupling constant to a solution change. K. B. Aubrecht, B. L. Lucht, D. B. Collum, *Organometallics* **1999**, *18*, 2981–2987.

## Low-Temperature, Catalyzed Growth of Indium Nitride Fibers from Azido-Indium Precursors\*\*

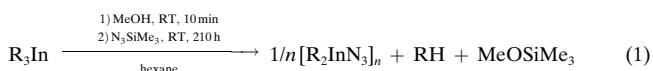
Sean D. Dingman, Nigam P. Rath, Paul D. Markowitz, Patrick C. Gibbons, and William E. Buhro\*

We have achieved low-temperature synthesis and crystallization of InN through precursor design and crystal-growth catalysis. The group III nitrides GaN, InN,  $\text{In}_n\text{Ga}_{1-n}\text{N}$ , and  $\text{Al}_n\text{Ga}_{1-n}\text{N}$  have recently acquired technological importance for blue/violet LED and laser diode applications.<sup>[1]</sup> However, InN begins decomposing with loss of  $\text{N}_2$  at low temperatures (427–550°C),<sup>[2,3]</sup> which makes the growth of crystalline InN-containing materials challenging. We now report, to our knowledge, the lowest-temperature synthesis of crystalline

InN, at 203°C, well below its decomposition range. The work demonstrates that catalysis effectively lowers crystallization barriers, allowing InN synthesis under the mild conditions of conventional, solution-phase chemistry. Catalyzed growth may thus offer new strategies for the preparation of crystalline, thermally unstable materials.

Typical chemical vapor deposition (CVD)<sup>[2]</sup> and melt<sup>[3]</sup> syntheses of InN and InN-containing alloys require temperatures within or above the InN decomposition range, and proceed with difficulty. Recently, crystalline InN has been grown by single-source CVD at the surprisingly low temperature of 350°C.<sup>[4]</sup> Efforts to prepare covalent, nonmolecular solids like InN at such low temperatures generally produce only amorphous products, due to the lack of active crystal-growth mechanisms.<sup>[5]</sup> We now report that InN crystal growth is activated at 203°C by a process in which nanometer-sized metal droplets serve as catalytic sites for crystalline fiber formation. The growth process appears to be directly analogous to the previously reported solution–liquid–solid (SLS) mechanism (see below).<sup>[5,6]</sup>

Azido precursor compounds have been previously used for CVD of group III nitrides;<sup>[2a,b,4,7]</sup> we have developed appropriate analogs for low-temperature, solution-phase growth of InN. The precursors  $i\text{Pr}_2\text{InN}_3$  (**1a**) and  $t\text{Bu}_2\text{InN}_3$  (**1b**) were prepared in one-pot procedures from the corresponding trialkylindanes via dialkylmethoxyindane intermediates [Eq. (1); R = *i*Pr (**1a**), *t*Bu (**1b**); 85–95% yields]. The



products are effectively insoluble in hydrocarbons at room temperature, but dissolve in Lewis-basic solvents such as pyridine and acetone. In the solid state, **1a** and **1b** are isostructural, ladderlike polymers (Figure 1).<sup>[8]</sup>

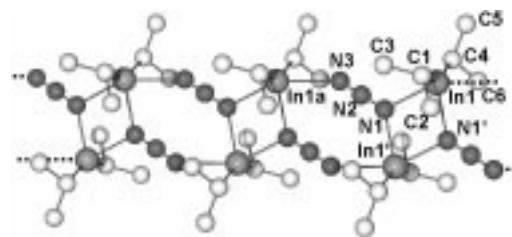


Figure 1. Ball-and-stick representation of the crystal structure of  $[i\text{Pr}_2\text{InN}_3]_n$  (**1a**).<sup>[8]</sup> Selected bond distances [Å] and angles [°]: In1–C1 2.166(2), In1–N1 2.296(2), In1–N1' 2.433(1), In1a–N3 2.655(3), N1–N2 1.194(2), N2–N3 1.138(3); C4–In1–C1 147.26(8), C1–In1–N1 105.21(7), C1–In1–N1' 99.07(7), In1–N1–In1' 107.66(6), C5–C4–In1 112.55(18), C4–In1–N1' 97.82(7), N1–In1–N1' 72.34(6), N3–N2–N1 178.9(2).

Reactions of the precursors **1a** or **1b** with the mild reductant<sup>[9]</sup> 1,1-dimethylhydrazine,  $\text{H}_2\text{NNMe}_2$ , produced crystalline InN. Thermolysis of **1a** in refluxing diisopropylbenzene (203°C) without  $\text{H}_2\text{NNMe}_2$  gave a gray-black precipitate with a broad powder X-ray diffraction (XRD) pattern (Figure 2a), indicating an amorphous structure. However, thermolysis of **1a** under the same conditions but with  $\text{H}_2\text{NNMe}_2$  gave black InN having an average XRD coherence length (approximate

[\*] Prof. W. E. Buhro, S. D. Dingman, P. D. Markowitz  
Department of Chemistry  
Washington University  
St. Louis, MO 63130-4899 (USA)  
Fax: (+1) 314-935-4481  
E-mail: buhro@wuchem.wustl.edu

Dr. N. P. Rath  
Department of Chemistry and Center for Molecular Electronics  
University of Missouri–St. Louis  
St. Louis, MO 63121 (USA)  
Prof. P. C. Gibbons  
Department of Physics  
Washington University  
St. Louis, MO 63130-4899 (USA)

[\*\*] This work was supported by the U.S. National Science Foundation (Grant CHE-9709104). We gratefully acknowledge assistance from Dr. W. R. Winchester with GC-MS and Dr. Couture with X-ray fluorescence studies.